Supplemental Material Content

1. Supplemental methods and materials
2. Supplemental table 1
3. Supplemental table 2
4. Supplemental table 3
5. Supplemental figure 1
6. Supplemental figure 2
7. Supplemental figure 3
8. Supplemental figure 4
9. Supplemental figure 5
10. Supplemental figure 6

Additional supplemental data containing proteomic data is provided online.

Supplemental data 1: Sample data LCM resource

Supplemental data 2: Protein data LCM resource

Supplemental data 3: Sample data PdX resource

Supplemental data 4: Protein data PdX resource

Supplemental data 5: Protein list mouse/human specific proteins identified from PdX

Supplemental data 6: Analysis differential expression tumor/stromal compartment

Supplemental data 7: Analysis differential prognostic expression stromal compartment

Supplemental data 8: Analysis differential prognostic expression tumor compartment

Supplemental materials and methods

Sample collection and processing

Approval from the Local Medical Ethical committee at the Amsterdam UMC, location VU University Medical Center was received for the Biobank (#14038). All patients gave informed consent for tissue sampling, clinical data analysis and molecular analysis. Consecutive snap-frozen tumor samples from January 2014 until November 2015 from the VU University Medical Center were evaluated for their quality and tumor percentage. The workflow is described in Figure 1A. After pathological evaluation, 16 samples were eligible for further LCM analysis and prepared as follows: frozen slides of 10μm thickness were applied on PEN foil slides (Leica, Germany). Sections were stained for 1 min with Mayers Hematoxylin, rinsed in RNAse free sterile water, and dehydrated in sequential concentrations of Ethanol and 100% Xylene. Dehydrated slides were stored at -80°C and thawed once for the LCM procedure. Additionally, unseparated bulk tumor of 11 matched and 5 unmatched samples were prepared for protein identification. This yielded a total of 21 PDAC samples.

Clinical parameters were collected prospectively and overall survival (OS; defined by registered death of the patient, or last visit to the clinic) and disease-free survival (DFS; defined as disease-free period between resection and registered recurrence of disease) were annotated. Two patients were censored for OS analysis and the differential analysis with short versus long survival, since they succumbed of complications after surgery, defined as a mortality within 60 days after surgery. Five patients were censored for DFS analysis due to different reasons; lost to follow up (n=1), mortality due to surgery (n=2), R2 resection (n=1), metastatic disease at time of resection (n=1). One patient in the cohort had stage IV disease. This patient was preoperatively predicted to suffer from duodenal adenocarcinoma, but pathological review showed PDAC. Since the liver metastasis was resected synchronously, the patient was not taken along for differential analysis comparing OS/DFS.

Laser capture microdissection procedure

LCM was performed on the Leica LMD7000 instrument (Leica-Microsystems, Wetzlar, Germany), for a total surface of $3x10^6$ μm^2 per compartment. Selected areas were captured in 0.1% RapiGest SF Surfactant (Waters, Milford, MA) and stored until further preparation. Samples were sonicated and reduced to a final concentration of 5mM dithiothreitol (DTT, Sigma-Aldrich, Saint Louis, MO) and 15mM iodoacetamide (IAA, Sigma-Aldrich, Saint Louis, MO). Sequencing-grade modified trypsin (Promega, Madison, WI) was added overnight to a final concentration of 7ng/μl. Digestion was stopped with acidification by trifluoroacetic acid (TFA). The peptide mixture was centrifuged and supernatant was transferred to a glass-lined MS/MS auto sampler vials. Samples were brought up to 20μl volume and stored at -80°C until further analysis.

Peptide preparations of PDX models and bulk tumor.

Animal work was performed in a previous study according to protocols approved by the animal experiment ethical committee at the Amsterdam UMC (location AMC, protocol DTB102348, LEX102774). NSG (Cg-Prkdc^{scid} Il2rg^{tm1Wjl}/SzJ) mice used for the experiments were bred in-house. Frozen tumors from 10 PDX models(1) were used for proteome analysis. A minimum of 100 mg of tissue was digested in lysis buffer (9M urea, 20mM HEPES pH 8.0, 1mM Na_3VO_4, 2.5mM $Na_4P_2O_7$, 1mM $Na_2C_3H_7PO_6$). 50μg of protein was loaded on a NuPAGE 4-12% gradient gel (Invitrogen, Carlsbad, CA). Proteins were digested and extracted according our whole-in-gel protocol described previously(2). In short, proteins were separated by gel-electrophoresis, fixed and stained with Coomassie Brilliant Blue solution. After reduction and alkylation, proteins were digested overnight with trypsin and extracted from the gel for further analysis. Bulk tumors were lysed and in-solution digestion was performed according to our laboratories protocol after reduction and alkylation(3). Digestion was inhibited by acidification with TFA and peptide eluates were desalted with 20 μl StageTips and peptides were stored in glass-lined autosampler vials(3) until measurement.

Nano-LC-MS/MS

Peptides were separated by an Ultimate 3000 nanoLC-MS/MS system (Dionex LC-Packings, Amsterdam, The Netherlands) equipped with a 40 cm × 75 µm ID fused silica column custom packed with 1.9 µm 120Å ReproSil Pur C18 aqua (Dr Maisch GMBH, Ammerbuch-Entringen, Germany). After injection, peptides were trapped at 6 µl/min on a 10 mm × 100 µm ID trap column packed with 5 µm 120 Å ReproSil Pur C18 aqua in 0.05% formic acid. Peptides were separated at 300 nl/min in a 10–40% gradient (buffer A: 0.5% acetic acid (Fisher Scientific, the Netherlands), buffer B: 80% ACN, 0.5% acetic acid) in 130 min (150 min inject-to-inject). Eluting peptides were ionized at a potential of +2 kVa into a Q Exactive HF mass spectrometer (Thermo Fisher, Bremen, Germany). Intact masses were measured at resolution 70.000 (at m/z 200) in the orbitrap using an AGC target value of 3E6 charges. The top 15 peptide signals (charge-states 2+ and higher) were submitted to MS/MS in the HCD (higher-energy collision) cell (1.6 amu isolation width, 25% normalized collision energy). MS/MS spectra were acquired at resolution 17.500 (at m/z 200) in the orbitrap using an AGC target value of 1E6 charges, a maxIT of 32 ms and an underfill ratio of 0.1%. Dynamic exclusion was applied with a repeat count of 1 and an exclusion time of 30 s.

Protein annotation and data analysis

MS/MS spectra were searched against the Swissprot FASTA file (*LCM data:* release march 2017, 42161 entries, canonical and isoforms. *PdX data:* uniprot_human_referenceproteome_2014_01_NO_fragments_42104entries.fasta (61552 entries); Uniprot_Mus_musculus_reference_proteome_2015_06_NO_FRAGMENTS_Canonical and isoforms _34331entries.fasta (42296 entries)) using MaxQuant 1.5.8.0.(4) Enzyme specificity was set to trypsin and up to two missed cleavages were allowed. Cysteine carboxamidomethylation (Cys, +57.021464 Da) was treated as fixed modification and methionine oxidation (Met,+15.994915 Da) and N-terminal acetylation (N-terminal, +42.010565 Da) as variable modifications. Peptide precursor ions were searched with a maximum mass deviation of 4.5 ppm and fragment ions with a maximum mass deviation of 20 ppm. Peptide and protein identifications were filtered at an FDR of 1% using the decoy database strategy. The minimal peptide

length was 7 amino acids. Proteins that could not be differentiated based on MS/MS spectra alone were grouped to protein groups (default MaxQuant settings). Searches were performed with the label-free quantification option selected.

A match-between-runs setting was implemented for analysis of low abundant proteins in the LCM database. Protein compartment specificity was correlated to mouse and human-specific proteins identified from PDX PDAC tumors (protein had to be uniquely mouse- or human-specific). Proteins had to be identified in 5 out of 10 samples for further selection in the species-specific list to reduce heterogeneity. Mouse genes were converted to human nomenclature for GSEA (See Supplemental Data 5). The mass spectrometry proteomics data have been deposited to the ProteomeXchange Consortium via the PRIDE(5) partner repository with the dataset identifier PXD011289 and PXD017393. One of the tumor samples (sample CC) showed low identifications and inadequate MS/MS data and was omitted from further analysis.

In silico validation of prognostic markers

Data of publicly available transcriptomic (microarray or RNAseq) datasets with survival data were downloaded from GEObase and each dataset was scaled to a mean of zero, with a standard deviation of 1 to allow meta-analysis. Univariate cox proportional hazard regression models were evaluated for genes of interest. The Metafor R package(6) was used to perform meta-analysis validation of identified prognostic markers. Combined hazard risk of proteins of interest and confidence intervals are reported if genes were identified in a minimum of 3 out of the 7 datasets.

Immunohistochemistry (IHC) validation of tissue microarrays (TMA)

Proteins of interest in both compartments (COL11A1, CALB2) were evaluated in two independent cohorts (N=95 and N=95) by staining TMAs of resected patients treated at the Pisa University Hospital. Written informed consent was obtained from all patients, and ethical approval was provided by the Ethics Committee of the Pisa University hospital (Pisa, Italy, date of approval: July 3, 2013 (file number 3909)). The PDAC TMA has been detailed previously(7) and represents an independent, non-overlapping cohort of patients. Assessment of IHC staining of COL11A1 was

performed in 3 tumor cores containing representatives regions of the desmoplastic reaction, and the expression was evaluated in relation to the stromal surface, as described previously(8). The cores with <1% positive staining were assigned a score of 0, while cores with positive staining between 1 and 10% were assigned a score of 1, cores with positive staining between 10% and 50% were assigned a score of 2, and cases with more than 50% positive staining were assigned a score of 3. Total variation in staining was defined by multiplying the number of positive cores (0-3) by the field's staining intensity (0-3), yielding a total score of 0-9. Samples were defined as "high COL11A1", when staining score was > 5; and "low COL11A1" when staining score was ≤ 5. Scoring for CALB2 was performed taking into account both the percentage of neoplastic cells stained and also the intensity of the staining (marked as 1+/2+/3+), as reported previously(9) The IHC score for each core was calculated separately and then an average of 3 cores was taken as the final score for each sample/patient. Samples were then categorised according to the median value and were defined as "high CALB2" when staining score was>median; and "low CALB2" when staining score ≤median.

The immunostaining was double-blind scored and correlated to clinical data by two researchers (NF and EG).

Western blot validation of EPHA2 expression

PANC1 (ATCC,Manassas, WI) was cultured in RPMI medium (Lonza, Switzerland). Capan-2 (ATCC, Manassas, WI) and Hs766t (ATCC, Manassas, WI) were cultured in DMEM medium (Lonza). Media was supplemented with 10% heat-inactivated fetal calf serum (Biowest, France) and 1% penicillin and streptomycin (Lonza). An immortalized pancreatic ductal cell line (HPDE, kindly supplied by dr. Tsao, Ontario, Canada(10)) was cultured in supplemented KGM medium (Lonza). Cell lysates were created with diluted 10x RIPA buffer (Abcam, UK) containing protease (cOmplete™ mini EDTA-free protease inhibitor cocktail tablets, Roche, Switzerland) and phosphatase inhibitors (1mM Na_3VO_4, 2.5mM $Na_4P_2O_7$, 1mM $Na_2C_3H_7PO_6$) according to manufacturer's protocol. The BCA protein estimation method (Pierce BCA protein assay kit, ThermoFisher, Waltham, MA) was used to evaluate protein yield. 20 μg of

protein was denatured with NuPAGE 4x LDS buffer (ThermoFisher, Waltham, MA), 10% DTT and heating. Separated Proteins were transferred to nitrocellulose membranes (EMDMillipore,Burlington, MA). Blocking was performed with 5% blotting-grade blocker non-fat dry milk (Biorad,Hercules, CA) in PBS and 0.1% Tween-20 (PBST). Primary antibodies were incubated in 5% BSA (Sigma-Aldrich, Saint Louis, MO) in PBST followed by secondary antibodies in 5% blocking buffer. Proteins were detected with SuperSignal West Pico Chemoluminescent substrate (ThermoFisher, Waltham, MA) and visualized by an Uvitec Imaging station (Cleaver Scientific, UK).

List of antibodies

Target	Conjugate	Antibody	Cat #	Supplier	Application
EPHA2	None	EphA2 (D4A2) XP Rabbit mAb	#6997	Cell Signaling Technology	WB
Phospho-EPHA2	None	Phospho-EphA2 (Tyr588) (D7X2L) Rabbit mAb	#12677	Cell Signaling Technology	WB
COL11A1	None	DMTX invascan	DMTX invascan	Oncomatryx	IHC
CALB	None	Anti-Calretinin mAb	Ab702	Abcam	IHC
Anti-rabbit	HRP	Anti-rabbit IgG, HRP-linked Antibody	#7074	Cell Signaling Technology	WB
Anti-rabbit	HRP	Goat-Anti-Rabbit IgG H&L	ab205718	Abcam	IHC

Stable *EPHA2* knockdown

Lentiviral plasmids were produced by transfecting HEK293T cells with *EPHA2* targeting pLKO.1 constructs (MISSION shRNA Library clone numbers TRCN0000006403 and TRCN0000197131) and a non-targeting sequence negative control (shc002). Transfected supernatant was collected after 48 hours and filtered through a 0.45μm filter (EMDMillipore, Burlington, MA). At 30% confluency, PDAC cell lines Capan-2 and Hs766t were transduced and subsequently selected after 48 hours with 2 μg/ml puromycin (Sigma-Aldrich, Saint Louis, MI). Knockdown efficiency was evaluated by Western blot as described above.

***In vitro* validation of drug target**

Cells were plated in 96-wells plates and allowed to attach overnight (PANC1 3000/well, Capan-2 5000/well, Hs766t 5000/well, HPDE 5000/well). Growth was evaluated over 72 hours in respect to the control at the start of the experiment. To evaluate proliferation, the doubling time was calculated. A specific EPHA2 inhibitor ALW-II-41-27 (APExBIO, Houston, TX) was evaluated for cytotoxic effect. DMSO was used as control. Effect on cell proliferation was quantified with Sulforhodamine B (SRB, Sigma Aldrich, Saint Louis, MO) staining of protein and was subsequently measured for absorbance at 492nm in the Synergy microplate reader (Biotek Cytation3 Cell Imaging Multi-Mode Reader, Waltham, MA) as described previously(11). Migration was evaluated by transwell migration after staining cells with fluorescent dye as described before(12). As attractant, FCS 1% or 1μg/mL EGF was used. Cells were pretreated with ALW-II-41-27 for 15 min prior to migration. Migration was evaluated every 2 minutes for 3 hours and values were controlled for background, and values from no-attractant controls were subtracted at each time point.

Statistical analysis

Data was analyzed with R (www.r-project.org, version 3.5.2.). Zeros were imputed based on normal distribution standard deviation of log transformed intensity data as

described previously before differential expression analysis. The highest measured intensity was used for further analysis from replicates. Unsupervised clustering was performed on z-score normalized data and Euclidean distance. Differential compartment expression was tested with paired statistics analysis (Limma R package)(13) and corrected for multiple testing by the Benjamini Hochberg equation. Differential expression between tumor and bulk tissue was performed by unpaired Limma statistics. Gene set analysis(14) was performed in R. Prognostic proteins were identified by unpaired limma statistics of a group comparison (short OS, <1 year versus longer OS, >2 years). Technical and biological replicates were evaluated with Pearson's correlation. Group comparison of correlations was tested with unpaired student's t-test. *In vitro* experimental comparisons were evaluated by paired or unpaired two-tailed student's t-test. For the migration assay, the AUC was calculated and tested with the Welch's t-test. Complete clinicopathological, follow-up, and recurrence data were available from prospectively maintained databases. Correlation of clinicopathological characteristics and gene panel expression (based on z-score group selection) with DFS/OS were evaluated with Kaplan-Meier curves and the Log-rank test. Prognostic value of IHC scoring was tested with uni- and multivariate analysis. Error-bars show the mean ± SEM. A P value of <.05 was considered statistically significant.

Supplemental Data/Figures

Supplemental Figure 1. Quality control of samples and LC-MS/MS data. A. Dot plot of tumor purity of samples used for analysis, LCM only (n=6), bulk only (n=5), both (n=10) (P = ns, two-way unpaired t-test between all groups)**. B.** Quality control with technical replicates shows high Pearson Coefficient correlation of replicates of tumor and stroma samples ($R^2 = 0.99$, $P < 0.0001$). **C.** Venn diagram of tumor and stromal proteins identified in each compartment. **D.** Heatmap of inter-sample correlation analysis. **E.** Bulk samples (n=16) correlate significantly better with stromal samples than tumor samples (two-way unpaired t-test $P < 0.0001$). **F.** Inter-sample correlation shows high inter-patient correlation in stroma compared to tumor samples (two-way unpaired t-test, $P<0.0001$). Data represent mean and SD. **G.** Dot plot showing specific tumor marker expression of EPCAM /KRT7/CDH1 in tumor and stromal areas (both n = 15) with low to none expression in stroma, indicating minimal contamination. Data represents mean and SD (paired-limma test, adjusted for multiple testing, $P<0.0001$).

Supplemental Figure 2. Correlation between proteomics and transcriptomics in PDAC PDXs. A. Scatter plot shows correlation for transcriptomics and proteomics data of 10 PDX models for PDAC. Data are visualized in bins and color count shows the frequency of genes for each bin. Regression line in red is estimated using the built-in lm() function in R. **B.** Correlation analysis of Enolase 1 (ENO1) protein counts with transcript levels. Dots denote individual PDXs. **C.** As panel B, for Proteasome 20S Subunit Beta 1(PSMB1) protein.

Supplemental Figure 3. Clustering to evaluate proteome subtypes. A. Protein clustering on most variable genes (top 500 proteins in tumor samples, top 50 proteins in stromal samples) showed two protein subclasses on either compartment. Samples were associated to known classifiers(15,17) by Z-score ranking. Correlation to known subtypes shows good correlation to previous established stromal subtypes. **B.** Kaplan-Meier curves of OS and DFS from proteome cohort of epithelial samples

(log-rank test, P = 0.11 and P = 0.323 respectively) and stroma (**C**) (log-rank test, P = 0.25 and P = 0.08 respectively for OS and DFS).

Supplemental Figure 4. Validation of prognostic markers in a second independent TMA cohort. A. Kaplan-Meier curves of high (red, n=45) or low (blue, n=50) expression of CALB2 in a second cohort shows significant correlation to OS (P < 0.009, median survival 17 versus 23 months, log-rank test). **B.** Kaplan-Meier curves of high (red, n=41) or low (blue, n=54) expression of COL11A1 shows no significant correlation the second validation cohort (P = ns, median survival 18 versus 22 months, log-rank test).

Supplemental Figure 5. EPHA2 inhibition as target in PDAC A. Expression of EGFR in bulk (n=16) and tumor (n=15) samples (limma-test corrected for multiple testing, adjusted P < 0.05). Data represents mean with SD. **B.** Western blot analysis of PDAC cell lines shows variance in EPHA2 expression. **C.** shRNA knock-down of EPHA2 control by Western Blot. shRNA 1 and shRNA 2 were chosen or further experiments. shRNAx were identified as non-functional shRNAs. **D.** Doubling time evaluation of Hs766t (P = non-significant, unpaired two-way t-test). Data represents mean with SEM (n = 3).**E.** Evaluation of detachment of Capan-2 with shRNAs against EPHA2 upon trypsinization. Cells were plated and attached overnight and detached by 1% trypsin. At time of evaluation, number of detached cells were counted and normalized to total number of cells. shRNA clone 2 detached slower (P = 0.013, unpaired two-way t-test). Data represents mean with SEM (n = 3).

Supplemental Figure 6. Full unedited western blots

Supplemental Table 1: Additional information for cohort
Supplemental Table 2: Clinicopathological information with samples
Supplemental Table 3: Clinical characteristics of two independent PDAC cohorts for TMAs

Supplemental methods and online extensive library.

Supplemental Data 1: Sample data LCM resource

Supplemental Data 2: Protein data LCM resource

Supplemental Data 3: Sample data PDX resource

Supplemental Data 4: Protein data PDX resource

Supplemental Data 5: Protein list mouse/human specific proteins identified from PDX

Supplemental Data 6: Analysis differential expression tumor/stromal compartment

Supplemental Data 7: Analysis differential prognostic expression stromal compartment

Supplemental Data 8: Analysis differential prognostic expression tumor compartment

Supplemental table 1

Clinicopathological information cohort			
	N	**Median (SE)**	**P value**
Overall survival	19	369 ± 189	
Age			
<69	9	353 ± 170	0.195
≥69	10	369 ± 248	
Sex			
Female	10	353 ± 51	0.241
Male	9	581 ± 385	
Disease stage			
Stage I-II	11	637 ± 241	0.846
Stage III-IV	8	323 ± 46	
Lymph nodes			0.946
N0	5	353 ± 67	
N1	8	581 ± 222	
N2	6	296 ± 80	
Tumor percentage (continious)			0.214
Adjuvant therapy			
No adjuvant therapy	8	292 ± 40	0.040*
Gemcitabine	11	730 ± 277	

Supplemental table 2

Patient	Bulk ID	Stroma ID	Tumor ID	Age at diagnosis	Sex	Tumor origin	Differentiation	T-stage	N-stage	M-stage	R	Stage (AJCC 8th edition)	Tumor percentage	Adjuvant therapy *	Recurrence	DFS (days)	Survival	OS (days)
PDAC1	**II**			58	f	PDAC	intermediate	2	1	0	1	2B	5-10%	yes	PD	529	D	740
PDAC2	**JJ**	**A**	**R**	65	f	PDAC	intermediate	3	0	0	1	2A	50%	yes	PD	595	D	885
PDAC3	**KK**	**B**	**S**	78	m	PDAC	intermediate	2	2	0	0	3	40%	no	PD	296	D	301
PDAC4	**LL**			54	m	PDAC	poor	2	2	0	2	3	5-10%	no	UN		D	243
PDAC5	**MM/NN**	**C**	**T**	50	f	PDAC	poor	3	0	0	1	2A	5-10%	partly	PD	105	D	143
PDAC6	**OO/PP**	**D**	**U**	77	f	PDAC	poor	3	0	0	1	2A	15%	no	PD	210	D	296
PDAC7	**QQ**	**E**	**V**	72	f	PDAC	intermediate	3	1	0	1	2B	70%	partly	PD	385	D	647
PDAC8		**F/G**	**W/X**	69	f	PDAC	poor	2	2	0	1	3	60%	yes	PD	351	D	374
PDAC9		**H**	**Y**	70	m	PDAC	well	3	1	0	1	2B	30%	yes	PD	737	A	1227
PDAC10		**I**	**Z**	80	m	PDAC	intermediate	2	1	0	1	2B	20%	no	UN		D, excluded	20
PDAC11	**RR**			63	f	PDAC	intermediate	2	0	0	1	1B	35%	partly	PD	339	D	358
PDAC12	**SS**	**J**	**AA**	73	m	PDAC	intermediate	2	2	0	1	3	35%	yes	NR		A	1217
PDAC13	**TT**	**K**	**BB**	60	m	PDAC	poor	2	1	0	0	2B	20%	yes	NR		A	1118
PDAC14	**UU**	**L**	**CC#**	75	m	PDAC	intermediate	1	0	0	1	1A	50%	no	NR		A	1037
PDAC15	**VV**			78	f	PDAC	poor	2	1	0	1	2B	5-10%	no	PD	235	D	309
PDAC16	**WW**	**M**	**DD**	67	m	PDAC	well	3	2	0	0	3	10%	no	PD	159	D	236
PDAC17		**N**	**EE**	64	m	PDAC	poor	2	1	0	1	2B	35%	no	UN		D, excluded	31
PDAC18		**O**	**FF**	73	m	PDAC	poor	2	1	0	1	2B	40%	partly	PD	167	D	329
PDAC19	**XX**	**P**	**GG**	71	m	PDAC	intermediate	3	2	0	1	3	35%	yes	PD	329	A	923
PDAC20	**YY**	**Q**	**HH**	67	f	PDAC	intermediate	2	1	0	1	2B	15%	no	PD	122	D	172
PDAC21	**ZZ**			67	m	PDAC	poor	2	1	1	0	4	70%	no	PD	335	D	589

PDAC: pancreatic ductal adenocarcinoma
PD: progressive disease
UN: unknown
NR: no recurrence
D: deceased
A: alive at last follow up
Excluded: death due to complication, excluded from survival analysis
* gemcitabine, yes = 6 cycles total regimen, < 6 cycles = partly, no = 0 cycles
#: failed sample

Supplemental table 3

Clinicopathological characteristics						
	First cohort			Second cohort		
Univariate analysis	**N (%)**	**OS months mean (95% CI)**	***p-value***	**N (%)**	**OS months (95% CI)**	***p-value***
No. patients	95 (100)	20.4 (18.0-22.8)		95 (100)	21.4 (19.6-22.9)	
Age, year - at time of diagnosis			*0.339*			*0.359*
> 65	36 (37.9)	19.06 (16.1-22.0)		41 (43.2)	22.7 (19.7-24.6)	
<= 65	59 (62.1)	21.22 (17.8-24.6)		54 (56.8)	20.5 (18.4-22.7)	
Gender			*0.016*			*0.476*
Female	42 (44.2)	23.69 (19.7-27.7)		44 (46.3)	20.1 (17.6-22.7)	
Male	53 (55.8)	17.79 (15.1-20.5)		51 (53.7)	22.5 (20.7-24.4)	
Vascular Infiltration			*0.012*			*0.065*
no	33 (34.7)	24.7 (19.9-29.5)		45 (47.4)	22.8 (20.2-25.4)	
yes	62 (65.3)	18.1 (15.6-20.6)		50 (52.6)	19.9 (17.9-21.8)	
Tumor grade			*0.033*			*0.054*
Grade 1-2	48 (51.5)	22.8 (19.1-26.7)		37 (38.9)	23.1 (20.2-26.4)	
Grade 3	47 (49.5)	17.9 (15.2-20.6)		58 (61.1)	20.0 (18.2-21.9)	
Resection Margin			*0.208*			*0.245*
no	50 (52.6)	15.06 (12.0-18.1)		56 (58.9)	22.4 (20.5-24.4)	
yes	45 (47.4)	21.66 (18.6-24.7)		58 (41.1)	19.2 (16.8-22.2)	
COL11A1			*0.016*			*0.530*
low	50 (52.6)	23.0 (19.3-26.7)		41 (43.2)	22.3 (10.1-24.5)	
high	45 (47.4)	17.5 (18.0-22.8)		54 (56.8)	20.4 (18.1-22.7)	
CALB2			*0.009*			*0.006*
low	47 (49.5)	23.6 (19.8-27.3)		45 (47.4)	24.3 (22.3-26.4)	
high	48 (51.5)	17.3 (14.5-20.0)		50 (52.6)	18.5 (16.2-20.7)	
Multivariate analysis	**df**	**Risk of death, HR (95% CI)**	***p-value***	**df**	**Risk of death, HR (95% CI)**	***p-value***
Gender (female vs. male)		0.53 (0.22-2.23)	*0.105*	/	/	/
Grading (3 vs. 1-2)		0.57 (0.21-0.85)	*0.037*		0.68 (0.33-1.55)	*0.108*
Vascular Infiltration (no vs. yes)		0.68 (0.27-2.10)	*0.144*		0.59 (0.27-1.19)	*0.084*
COL11A1 (low vs. high)		0.92 (0.76-1.87)	*0.312*	/	/	/
CALB2 (low vs. high)		0.32 (0.21-0.61)	*0.004*		0.36 (0.25-0.67)	*0.008*

Multivariate analysis (when P<=0.1 at univariate)

Supplemental Figure 1

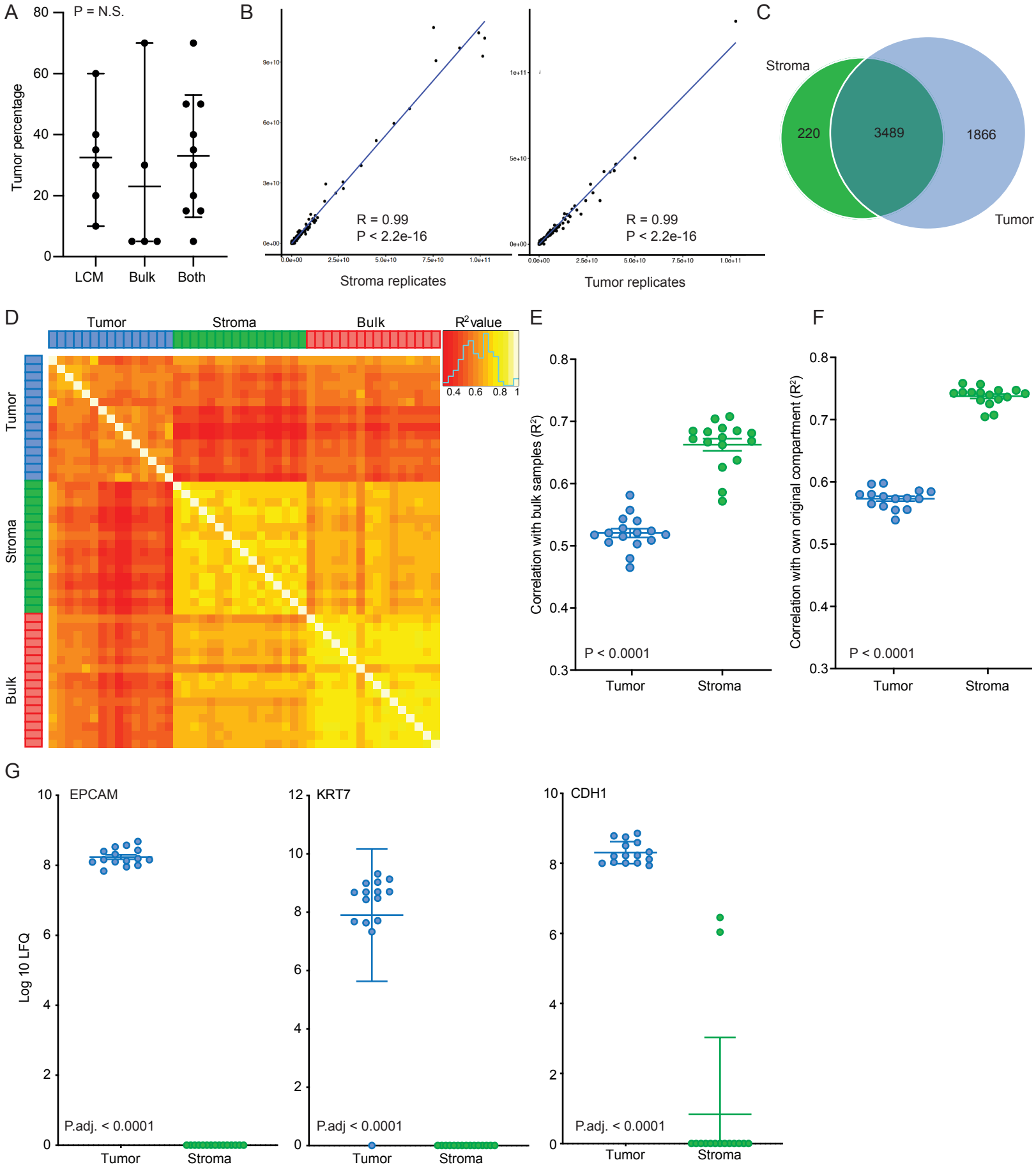

Supplemental Figure 1. Quality control of samples and LC-MS/MS data. A. Dot plot of tumor purity of samples used for analysis, LCM only (n=6), bulk only (n=5), both (n=10) (P = ns, two-way unpaired t-test between all groups). B. Quality control with technical replicates shows high Pearson Coefficient correlation of replicates of tumor and stroma samples (R2 = 0.99, P < 0.0001). C. Venn diagram of tumor and stromal proteins identified in each compartment. D. Heatmap of inter-sample correlation analysis. E. Bulk samples (n=16) correlate significantly better with stromal samples than tumor samples (two-way unpaired t-test P < 0.0001). F. Inter-sample correlation shows high inter-patient correlation in stroma compared to tumor samples (two-way unpaired t-test, P<0.0001). Data represent mean and SD. G. Dot plot showing specific tumor marker expression of EPCAM /KRT7/CDH1 in tumor and stromal areas (both n = 15) with low to none expression in stroma, indicating minimal contamination. Data represents mean and SD (paired-limma test, adjusted for multiple testing, P<0.0001).

Supplemental Figure 2

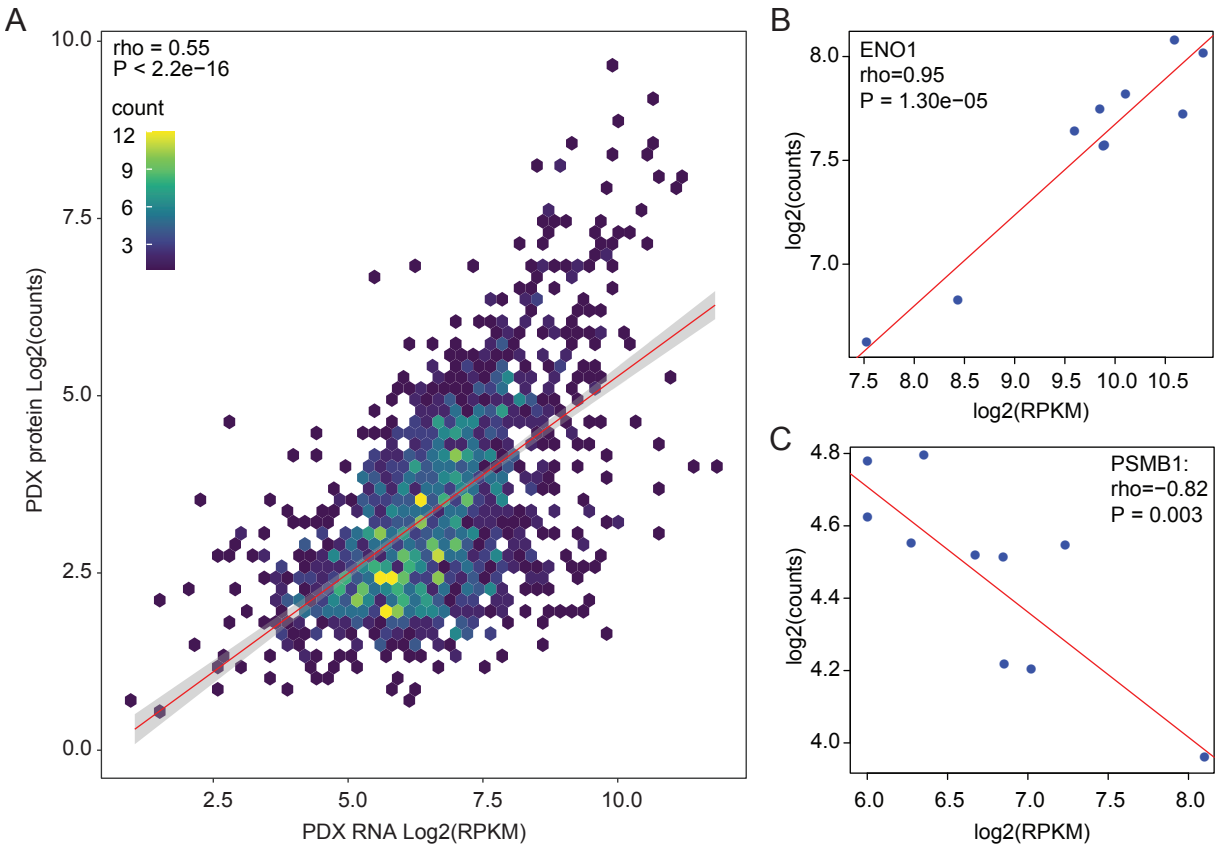

Supplemental Figure 2. Correlation between proteomics and transcriptomics in PDAC PDXs. A. Scatter plot shows correlation for transcriptomics and proteomics data of 10 PDX models for PDAC. Data are visualized in bins and color count shows the frequency of genes for each bin. Regression line in red is estimated using the built-in lm() function in R. B. Correlation analysis of Enolase 1 (ENO1) protein counts with transcript levels. Dots denote individual PDXs. C. As panel B, for Proteasome 20S Subunit Beta 1(PSMB1) protein.

Supplemental Figure 3

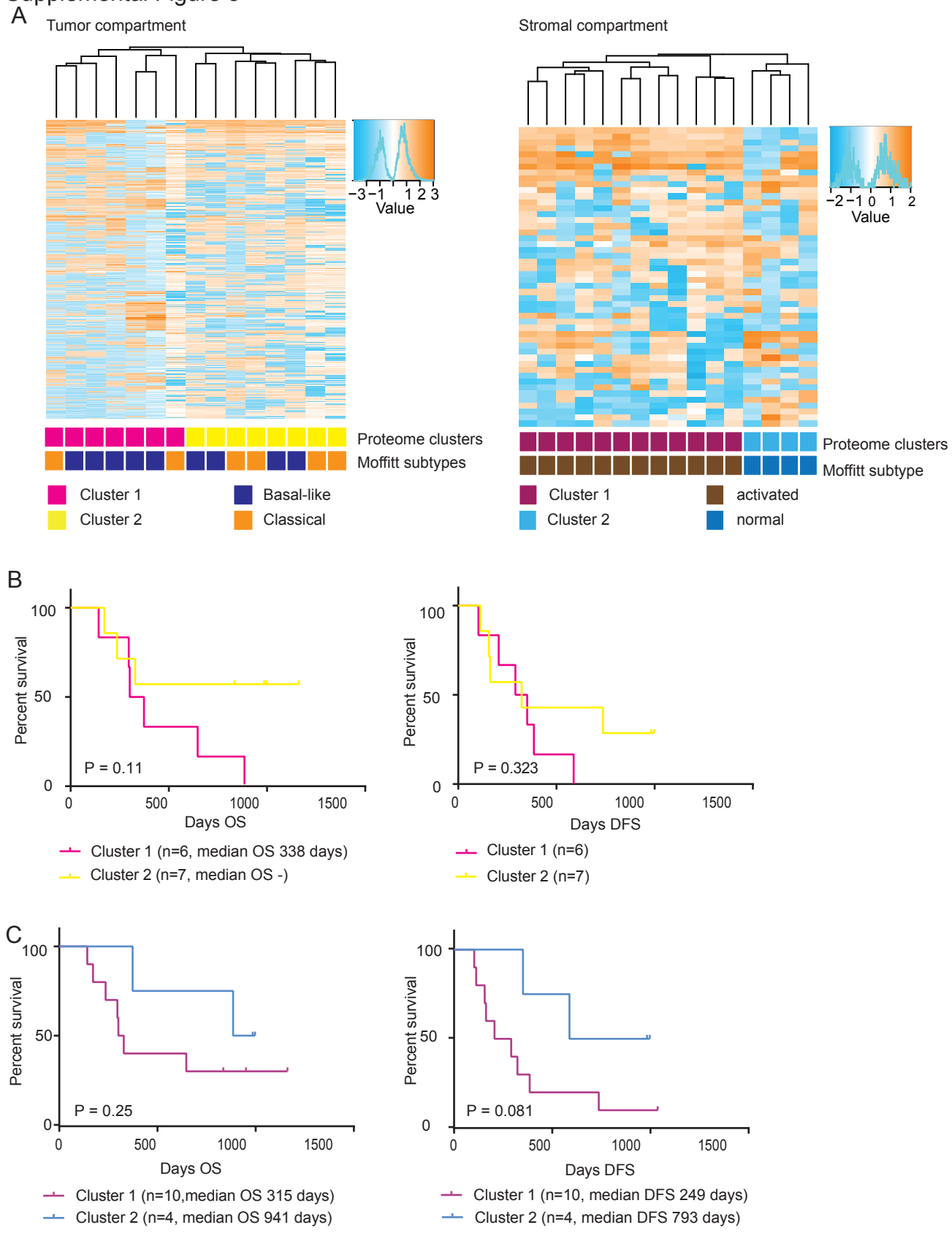

Supplemental Figure 3. Clustering to evaluate proteome subtypes. A. Protein clustering on most variable genes (top 500 proteins in tumor samples, top 50 proteins in stromal samples) showed two protein subclasses on either compartment. Samples were associated to known classifiers(15,17) by Z-score ranking. Correlation to known subtypes shows good correlation to previous established stromal subtypes. B. Kaplan-Meier curves of OS and DFS from proteome cohort of epithelial samples (log-rank test, P = 0.11 and P = 0.323 respectively) and stroma (C) (log-rank test, P = 0.25 and P = 0.08 respectively for OS and DFS).

Supplemental Figure 4

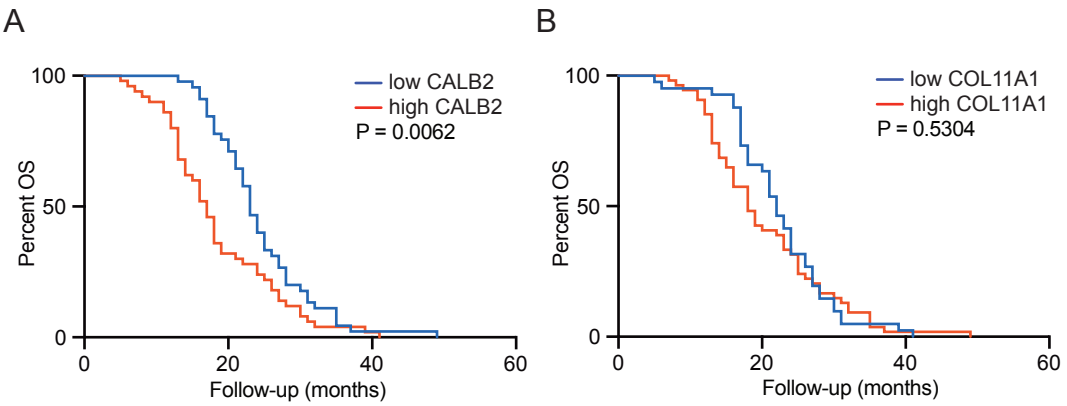

Supplemental Figure 4. Validation of prognostic markers in a second independent TMA cohort. A. Kaplan-Meier curves of high (red, n=45) or low (blue, n=50) expression of CALB2 in a second cohort shows significant correlation to OS ($P < 0.009$, median survival 17 versus 23 months, log-rank test). B. Kaplan-Meier curves of high (red, n=41) or low (blue, n=54) expression of COL11A1 shows no significant correlation the second validation cohort (P = ns, median survival 18 versus 22 months, log-rank test).

Supplemental Figure 5

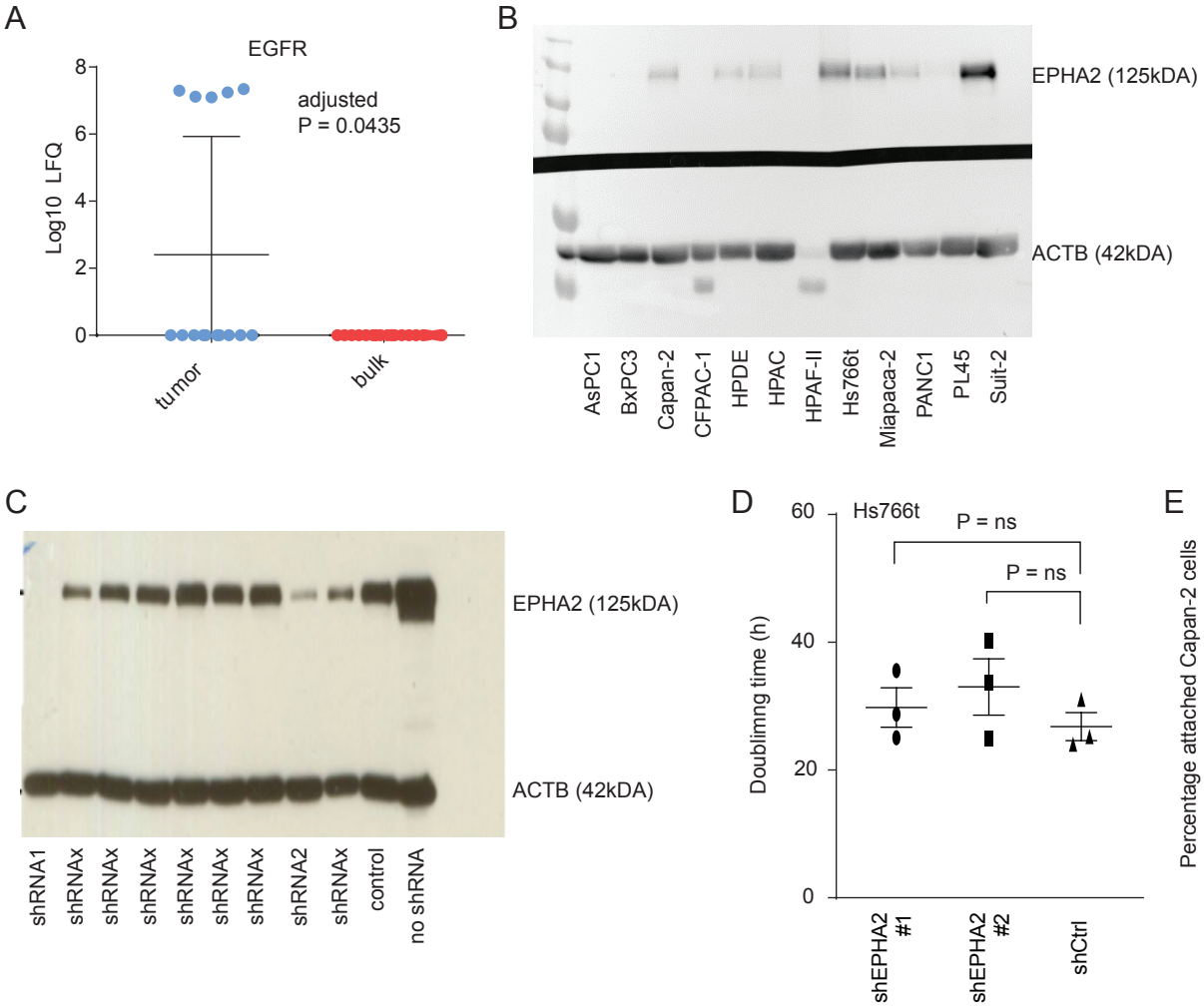

Supplemental Figure 5. EPHA2 inhibition as target in PDAC A. Expression of EGFR in bulk (n=16) and tumor (n=15) samples (limma-test corrected for multiple testing, adjusted P < 0.05). Data represents mean with SD. B. Western blot analysis of PDAC cell lines shows variance in EPHA2 expression. C. shRNA knock-down of EPHA2 control by Western Blot. shRNA 1 and shRNA 2 were chosen or further experiments. shRNAx were identified as non-functional shRNAs. D. Doubling time evaluation of Hs766t (P = non-significant, unpaired two-way t-test). Data represents mean with SEM (n = 3).E. Evaluation of detachment of Capan-2 with shRNAs against EPHA2 upon trypsinization. Cells were plated and attached overnight and detached by 1% trypsin. At time of evaluation, number of detached cells were counted and normalized to total number of cells. shRNA clone 2 detached slower (P = 0.013, unpaired two-way t-test). Data represents mean with SEM (n = 3).

Full unedited western blot analysis of Figure 5D

Lane
1. CAPAN control
2. CAPAN 2hr
3. CAPAN 24 hr
4. Hs766t control
5. Hs744t 2hr
6. Hs766t 24hr

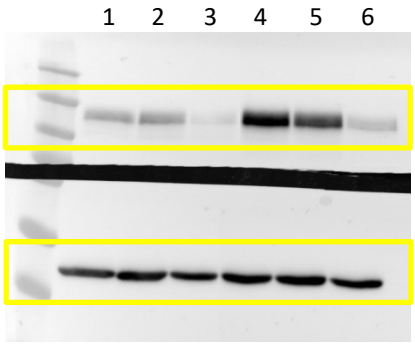

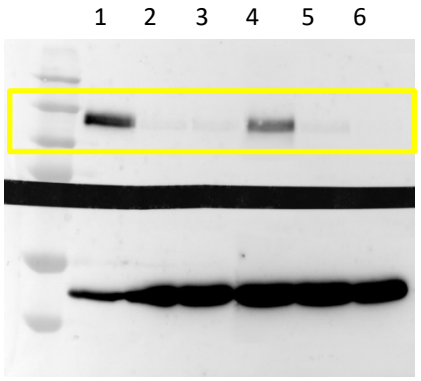

Lane
1. HPDE control
2. HDPE 2hr
3. HPDE 24 hr
4. PANC1 control
5. PANC1 2hr
6. PANC1 24hr

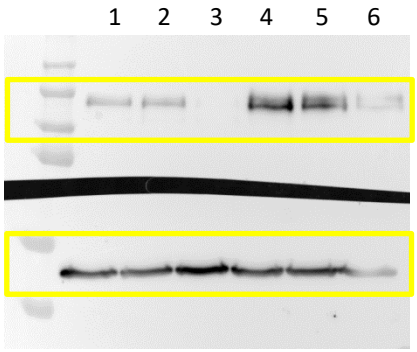

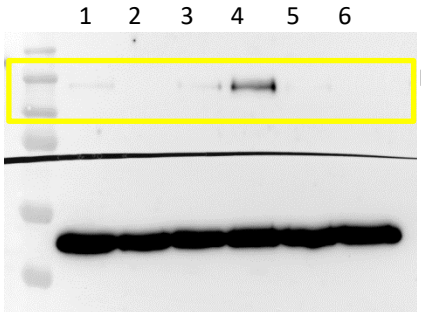

References methods

1. Damhofer H, et al. Establishment of patient-derived xenograft models and cell lines for malignancies of the upper gastrointestinal tract. *J Transl Med*. 2015;13(1):1-14.
2. Piersma SR, Warmoes MO, de Wit M, de Reus I, Knol JC, Jiménez CR. Whole gel processing procedure for GeLC-MS/MS based proteomics. *Proteome Sci*. 2013;11(1):17.
3. Piersma SR, et al. Feasibility of label-free phosphoproteomics and application to base-line signaling of colorectal cancer cell lines. *J Proteomics*. 2015;127:247-258.
4. Cox J, Mann M. MaxQuant enables high peptide identification rates, individualized p.p.b.-range mass accuracies and proteome-wide protein quantification. *Nat Biotechnol*. 2008;26(12):1367-1372.
5. Vizcaíno JA, et al. 2016 update of the PRIDE database and its related tools. *Nucleic Acids Res*. 2016;44(D1):D447-D456.
6. Viechtbauer W. Conducting meta-analyses in R with the metafor. *J Stat Softw*. 2010;36(3):1-48.
7. Le Large TYS, et al. Proteomic analysis of gemcitabine- resistant pancreatic cancer cells reveals that microtubule-associated protein 2 upregulation associates with taxane treatment. *Ther Adv Med Oncol*. 2019;11:1-17.
8. García-Pravia C, et al. Overexpression of COL11A1 by Cancer-Associated Fibroblasts: Clinical Relevance of a Stromal Marker in Pancreatic Cancer. *PLoS One*. 2013;8(10):1-13.
9. Thapa B, et al. Calretinin but not caveolin-1 correlates with tumour histology and survival in malignant mesothelioma. *Pathology*. 2016;48(7):660-665.
10. Furukawa T, Duguid W, Rosenberg L, Viallet J, Galloway D, Tsao M. Long-term culture and immortalization of epithelial cells from normal adult human pancreatic ducts transfected by the E6E7 gene of human papilloma virus 16. *Am J Pathol*. 1996;148(6):1763-1770.
11. Sciarrillo R, et al. Splicing modulation as novel therapeutic strategy against diffuse malignant peritoneal mesothelioma. *EBioMedicine*. 2019;39:215-225.
12. Ebbing EA, et al. Esophageal Adenocarcinoma Cells and Xenograft Tumors

Exposed to Erb-b2 Receptor Tyrosine Kinase 2 and 3 Inhibitors Activate Transforming Growth Factor Beta Signaling, Which Induces Epithelial to Mesenchymal Transition. *Gastroenterology*. 2017;153(1):63-76.e14.

13. Ritchie ME, et al. Limma powers differential expression analyses for RNA-sequencing and microarray studies. *Nucleic Acids Res*. 2015;43(7):e47.
14. Subramanian A, et al. Gene set enrichment analysis: A knowledge-based approach for interpreting genome-wide expression profiles. *Proc Natl Acad Sci U S A*. 2005;102(43):15545-15550.